Growth and spectroscopic characterization of a new 6.2 at.% Yb-doped LGSB crystal

M. GRECULEASA, F. VOICU, S. HAU, C. GHEORGHE, L. GHEORGHE*
National Institute for Laser, Plasma and Radiation Physics, Laboratory of Solid-State Quantum Electronics, Magurele, 077125, Ilfov, Romania

A high-quality Yb:LGSB crystal was successfully grown by the Czochralski method from the starting melt composition $La_{0.678}Yb_{0.08}Gd_{0.492}Sc_{2.75}(BO_3)_4$. The chemical composition of the Yb:LGSB grown crystal was calculated to be $La_{0.682}Yb_{0.062}Gd_{0.374}Sc_{2.882}(BO_3)_4$, corresponding to a Yb^{3+} concentration of 6.2 at.%. The XRPD spectrum revealed the existence of a single trigonal phase (space group R32) and the unit cell parameters were determined to be a= 9.798(1) Å and c= 7.961(2) Å. The spectroscopic investigations indicate that laser emission in the ~1.03 μm range can be successfully generated by the 6.2 at% Yb:LGSB crystal.

(Received November 15, 2024; accepted December 2, 2024)

Keywords: Crystal, Laser, Czochralski

1. Introduction

The development of advanced laser crystals has led to significant progress in the field of photonics, particularly in the realization of new laser systems, making them valuable in areas such as materials science [1-5], laser processing [6], ultrafast optics [7,8], telecommunications [9], medical procedures [10], and scientific research [11-13]. Among these crystals, ytterbium (Yb)-doped laser crystals have gained considerable attention, being more suitable for high-efficiency and high-average-power laser emission. The main advantage of Yb^{3+} ions lies in their simple electronic structure, comprising only two manifolds: the ground state manifold $^2F_{7/2}$ and the excited state manifold $^2F_{5/2}$. This energy level scheme circumvents the parasitic effects of up-conversion, cross-relaxation, and excited-state absorption, which are common in Nd-doped crystals due to the presence of additional higher excited states. These unwanted effects give rise to issues regarding the thermal load because the primary relaxation pathways from the higher excited states are non-radiative. Furthermore, they can impact the gain by inducing a strong depopulation of the $^4F_{3/2}$ level, which is implicated in the laser population inversion. Another advantage of Yb^{3+} ion is given by the very low quantum defect, typically around 5% when pumped at 980 nm and lasing near 1030 nm, depending on the host crystal. However, the low quantum defect also leads to a quasi-three-level scheme in the gain medium, requiring a more careful laser design to manage ground-state absorption due to the partial overlap between the ground state and the lower laser level. In the context of self-frequency doubling (SFD) lasers, both the host crystal and the activator ion must be carefully selected to have an efficient coupling between the frequency-doubling effects and laser emission. Therefore, the symmetry of the host crystal must not include an inversion center in order to allow second-order nonlinear optical (NLO) properties and, at the same time, must be suitable for doping with active ions, which determines that both the mature laser crystal (such as YAG or YVO_4) and nonlinear optical crystals (like KDP, KTP, LBO, and BBO) cannot be used as SFD crystals. Yttrium aluminum borate (YAB) is known as a good NLO crystal and also as an excellent host crystal for Yb^{3+} and Nd^{3+} ions. In the case of the Nd^{3+} doped YAB crystal (Nd:YAB), the strong absorption peak at ~ 532 nm is detrimental to the efficient green SFD laser converted from 1.06 μm fundamental emission [14]. For this reason, to date, watt-level SFD green laser emission has only been obtained from the Yb^{3+} doped YAB crystal (Yb:YAB) [15]. However, the main disadvantage of the YAB crystal is given by its incongruent melting which imposes the growth by the flux method, thus making it difficult to grow large size and high-quality crystals. To overcome this drawback, research has focused on the development of scandium-based borates with huntite structure (space group R32) that can be grown by the Czochralski method. In the last years, NLO and bifunctional crystals of $La_xGd_xSc_{4-x-y}(BO_3)_4$ – LGSB and $La_xY_xSc_{4-x-y}(BO_3)_4$ – LYSB pure [16-19] and single-doped with Yb^{3+} [20, 21], Nd^{3+} [22-26], and Pr^{3+} [27] were successfully grown by the Czochralski method. Herein, we present the growth by the Czochralski method and spectroscopic characterization of 6.2 at.% Yb^{3+}-doped LGSB crystal as a new potential laser and SFD medium, being the continuation of our previous work [20].

2. Experimental techniques

2.1. Crystal growth

The 8 at.% Yb:LGSB crystal (starting melt composition) was grown by the Czochralski method using an induction heating ADL-MP crystal growth equipment.

The polycrystalline Yb:LGSB compound was synthesized by the solid-state reaction method, according to the following chemical equation:

$$0.339\ La_2O_3 + 0.04\ Yb_2O_3 + 0.246\ Gd_2O_3 + 1.375\ Sc_2O_3 + 2B_2O_3 \rightarrow La_{0.678}\ Yb_{0.08}\ Gd_{0.492}\ Sc_{2.75}\ (BO_3)_4$$

The raw materials used were La_2O_3, Yb_2O_3, Gd_2O_3, Sc_2O_3 with purities of 99.999% and B_2O_3 with 99.98%. Also, a 5% excess of B_2O_3 relative to stoichiometric amounts was added to compensate for evaporation losses. La_2O_3, Yb_2O_3, Gd_2O_3, and Sc_2O_3 powders were preheated in air at 1000 °C for 12 hours. Following this, all raw materials were weighed precisely according to the chemical equation and carefully grounded and mixed in an agate mortar. The resulting powder mixture was then pressed into tablets and heated up in air at 1300 °C for 24 hours. A special thermal setup was used for the growth of 8 at.% Yb:LGSB crystals by the Czochralski method [16]. The growth was performed using iridium crucibles with dimensions of 30 mm in height and diameter, under N_2 atmosphere. More details on the crystal growth process can be found in our previous work [16-18].

2.2. X-ray diffraction

X-ray powder diffraction (XRPD) measurements were conducted at room temperature using a PANalytical Empyrean diffractometer in Bragg-Brentano geometry, equipped with a copper (Cu) X-ray source ($K\alpha_1$ radiation, $\lambda = 1.5406$ Å). The 2θ angle was scanned from 10° to 70° with a step size of 0.01°. Phase identification was performed using X'Pert HighScore Plus software.

2.3. Spectroscopic characterization

Absorption and emission spectra were measured at 300 K using a Jarell-Ash monochromator. The detection setup included S1 photomultipliers paired with lock-in amplifiers connected to computers. Emission spectra were recorded under excitation from a laser diode with emission centered at 885 nm.

3. Results and discussion

3.1. Crystal growth

Yb:LGSB crystal was grown by the Czochralski method from the starting melt composition $La_{0.682}\ Yb_{0.062}\ Gd_{0.374}\ Sc_{2.882}\ (BO_3)_4$, using a ***c***-cut oriented LGSB seed. The growth parameters, i.e. the pulling and rotation rates, were set to 2 mm/h and 10 rpm, respectively, and kept constant during the growth process. After the growth, the crystal was cooled to room temperate with a slow cooling rate of 22 °C/h to prevent cracking caused by the temperature variation. As can be seen in Fig. 1, the as-grown crystal is highly transparent, free of visible defects like cracks and inclusions, and has well-developed facets characteristic to huntite-type crystals grown along the ***c***-axis. The starting melt composition of $La_{0.678}Yb_{0.08}Gd_{0.492}Sc_{2.75}(BO_3)_4$, corresponding to a Yb^{3+} doping concentration of 8 at.%, together with the optimized growth parameters, allowed us to obtain a higher quality Yb:LGSB crystal than that obtained in our previous work [20], at least in terms of visible defects and transparency.

Fig. 1. As-grown Yb:LGSB crystal (color online)

3.2. Compositional and X-ray characterization

The chemical composition of the Yb:LGSB crystal was calculated from the composition of the starting melt using the segregation coefficients (the ratios between the concentrations of atoms in the growing crystal and those in the starting melt) for La^{3+}, Gd^{3+}, Sc^{3+}, and Yb^{3+} in the LGSB crystal matrix [16, 20]. Based on this consideration, the composition of the grown crystal was determined to be $La_{0.682}\ Yb_{0.062}\ Gd_{0.374}\ Sc_{2.882}\ (BO_3)_4$. Therefore, the concentration of Yb^{3+} ions in the grown crystal was 6.2 at.%.

The XRPD spectrum of the 6.2 at.% Yb:LGSB crystal is presented in Fig. 2 together with the reference pattern of the pure LGSB crystal [28]. As can be observed, the spectrum is in perfect agreement with the reference, demonstrating the presence of the trigonal phase (space group R32) as a single phase. The unit cell parameters were determined to be a= 9.798(1) Å and c= 7.961(2) Å, corresponding to a unit cell volume of 661.90 $Å^3$.

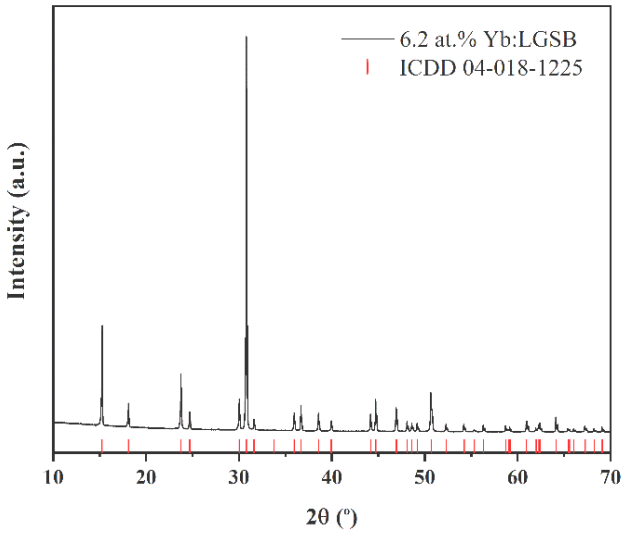

Fig. 2. XRPD pattern at room temperature of the 6.2 at.% Yb:LGSB crystal. Vertical lines indicate reference peaks from the ICDD 04-018-1225 pattern for the LGSB phase [28] (color online)

3.3. Spectroscopic properties

Absorption and emission spectra of 6.2 at% Yb:LGSB crystal were measured at room temperature for both σ (**E**⊥***c***) and π (**E**∥***c***) polarizations, where ***E*** is the electric field vector and ***c*** represents the direction of the crystallographic ***c***-axis of investigated samples. Based on these measurements, the absorption cross-sections (σ_{abs}) were determined using the formula $\sigma_{abs}= k(\lambda)/N$, where $k(\lambda)$ is the absorption coefficient in cm^{-1} and N is the number of ytterbium ions per cm^3, and the emission cross-sections (σ_{em}) were obtained by using the Fuchtbauer-Ladenburg method [29]. The obtained results are shown in Figs. 3a and 3b.

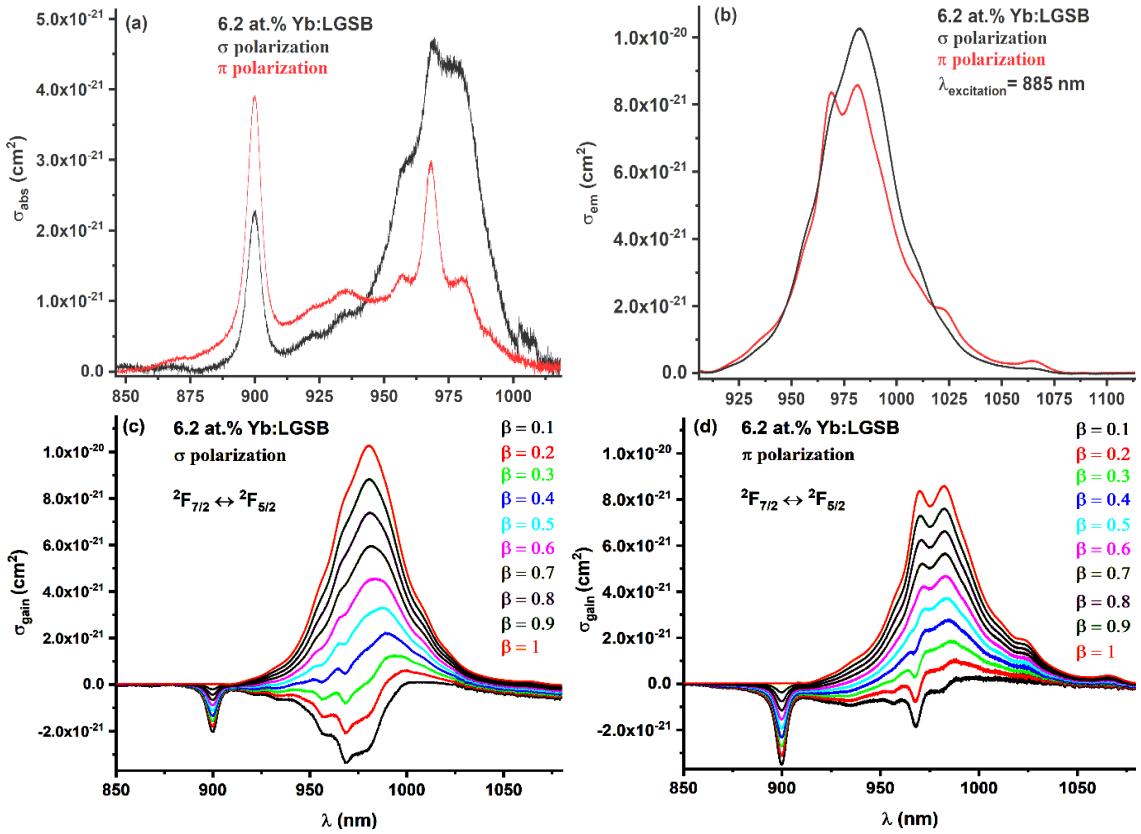

Fig. 3. Absorption (a) and emission (b) cross-sections of Yb^{3+} ions in 6.2 at% Yb:LGSB crystal. Gain cross-sections of Yb^{3+} ions in 6.2 at% Yb:LGSB crystal in σ (c) and π (d) polarizations (color online)

By using the equation $\sigma_g(\lambda) = \beta\sigma_{em}(\lambda) - (1 - \beta)\sigma_{abs}(\lambda)$, where β is the inversion population ratio, the gain cross-sections (σ_g) in both polarizations were also determined (Figs. 3c and 3d). According to these results, laser emission in the ~1.03 μm range, especially with π polarization, can be successfully generated by the newly discovered 6.2 at% Yb:LGSB crystal, which constitutes the next step of our research in the field of Yb:LGSB-type crystals.

4. Conclusions

A high-quality Yb:LGSB crystal was successfully grown by the Czochralski method from the starting melt composition $La_{0.682}Yb_{0.062}Gd_{0.374}Sc_{2.882}(BO_3)_4$. The crystal was grown along the ***c***-axis direction using constant pulling and rotation rates of 2 mm/h and 10 rpm, respectively. The as-grown crystal displayed high transparency, free of visible defects like cracks or inclusions, and exhibited well-defined facets typical of huntite-type crystals. The improved quality over prior growths is attributed to the starting melt composition and refined growth parameters. The chemical composition of the Yb:LGSB grown crystal was calculated to be $La_{0.682}Yb_{0.062}Gd_{0.374}Sc_{2.882}(BO_3)_4$, corresponding to a Yb^{3+} concentration of 6.2 at.%. The XRPD spectrum revealed the existence of a single trigonal phase (space group R32) and the unit cell parameters were determined to be a= 9.798(1) Å and c= 7.961(2) Å. The spectroscopic investigations indicate that laser emission in the ~1.03 μm range can be successfully generated by the 6.2 at% Yb:LGSB crystal.

Acknowledgments

This work was supported by the Romanian Ministry of Research, Innovation and Digitalization through project 30N/2023 within program NUCLEU LAPLAS VII.

References

[1] W. Ruan, M. Xie, J. Qiu, Y. Xian, X. Zhang, Optoelectron. Adv. Mat. **17**(7-8), 329 (2023).
[2] G. Croitoru, F. Jipa, M. Greculeasa, A. Broasca, F. Voicu, L. Gheorghe, N. Pavel, Materials **17**(8), 1758 (2024).
[3] C. Gheorghe, S. Hau, L. Gheorghe, A. Broasca, M. Greculeasa, F. Voicu, G. Stanciu, M. Enculescu, Opt. Mater. **150**, 115286 (2024).
[4] C. Gheorghe, S. Hau, G. Stanciu, D. Avram, A. Broasca, L. Gheorghe, J. Alloy. Compd. **922**,166178 (2022).
[5] H. M. Trung, B. T. Minh, N. L. Thai, H. Y. Lee, Optoelectron. Adv. Mat. **17**(9-10), 461 (2023).
[6] R. Indhu, S. Radha, E. Manikandan, B. S. Sreeja, J. Optoelectron. Adv. M. **22**(7-8), 400 (2020).
[7] M. Porębski, M. Kowalczyk, L. Gheorghe, M. Greculeasa, A. Broasca, F. Voicu, J. Sotor, The European Conference on Lasers and Electro-Optics. Optica Publishing Group, 2019. p. ca_p_24
[8] P. M. Donaldson, G. M. Greetham, C. T Middleton, B. M. Luther, M. T Zanni, P. Hamm, A. T. Krummel, Acc. Chem. Res. **56**(15), 2062 (2023).
[9] X. Huang, S. Liang, L. Xu, D. J. Richardson, Y. Jung, IEEE Photonics Technol. Lett. **36**(12), 791 (2024).
[10] T. Pu, J. Wang, W. Wang, B. Jing, Q. Han, C. Li, H. Liang, H., Opt. Lett. **49**, 3612 (2024).
[11] C. Gheorghe, S. Hau, L. Gheorghe, F. Voicu, M. Greculeasa, A. Broasca, G. Stanciu, Materials **16**(1), 269 (2023).
[12] S. Hau, C. Gheorghe, L. Gheorghe, F. Voicu, M. Greculeasa, G. Stanciu, A. Broasca, M. Enculescu, J. Alloy. Compd. **799**, 288 (2019).
[13] J. W. Zhang, M. B. Li, N. Zhang, W. Z. Jiang, Optoelectron. Adv. Mat. **8** (11-12), 998 (2014).
[14] H. Yu, Z. Pan, H. Zhang, J. Wang, J. Materiomics **2**(1), 55 (2016).
[15] P. Dekker, J. M. Dawes, J. A. Piper, Y. Liu, J. Wang, Optics Communications **195**(5-6), 432 (2001).
[16] L. Gheorghe, F. Khaled, A. Achim, F. Voicu, P. Loiseau, G. Aka, Cryst. Growth Des. **16**(6), 3473 (2016).
[17] L. Gheorghe, M. Greculeasa, A. Broasca, F. Voicu, G. Stanciu, K. N. Belikov, E. Yu. Bryleva, O. Gaiduk, ACS Appl. Mater. Interfaces **11**(23), 20987 (2019).
[18] A. Broasca, M. Greculeasa, F. Voicu, C. Gheorghe, L. Gheorghe, Crystals **13**(2), 169 (2023).
[19] A. Broasca, L. Gheorghe, M. Greculeasa, F. Voicu, G. Stanciu, S. Hau, C. Gheorghe, G. Croitoru, N. Pavel, Laser Congress 2019 (ASSL, LAC, LS&C), OSA Technical Digest, paper JM5A.40 (2019). (Optica Publishing Group, 2019).
[20] F. Khaled, P. Loiseau, F. Voicu, A. Achim, S. Hau, C. Gheorghe, G. Croitoru, N. Pavel, L. Gheorghe, G. Aka, J. Alloy. Compd. **688**, 510 (2016).
[21] A. Broasca, M. Greculeasa, F. Voicu, S. Hau, G. Croitoru, C. Gheorghe, N. Pavel, L. Gheorghe, J. Alloy. Compd. **844**, 156143 (2020).
[22] C. A. Brandus, S. Hau, A. Broasca, M. Greculeasa, F. M. Voicu, C. Gheorghe, L. Gheorghe, T. Dascalu, Materials **12**(12), 2005 (2019).
[23] M. Greculeasa, A. Broasca, F. Voicu, S. Hau, G. Croitoru, G. Stanciu, C. Gheorghe, N. Pavel, L. Gheorghe, Opt. Laser. Technol. **131**, 106433 (2020).
[24] C. A. Brandus, M. Greculeasa, A. Broasca, F. Voicu, L. Gheorghe, N. Pavel, Opt. Mater. Express 11(3), 685 (2021)
[25] A. Broasca, M. Greculeasa, F. Voicu, G. Stanciu, S. Hau, C. Gheorghe, C. A. Brandus, N. Pavel, M. Enculescu, L. Gheorghe, Opt. Mat. **123**, 111832 (2022).
[26] A. Broasca, M. Greculeasa, F. Voicu, S. Hau, C. Gheorghe, G. Croitoru, N. Pavel, G. Stanciu, A. Petris, P. Gheorghe, F. Albota, A. Serban, L. Gheorghe, J. Am. Chem. Soc. **146**(3), 2196 (2024).
[27] A. Broasca, M. Greculeasa, F. Voicu, G. Stanciu, S. Hau, C. Gheorghe, L. Gheorghe, J. Alloy. Compd. **908**, 164633 (2022).

[28] X. Xu, N. Ye, J. Cryst. Growth **324**(1), 304 (2011).

[29] W. Krupke, IEEE J. Quantum Electron. **10**(4), 450 (1974).

*Corresponding author: lucian.gheorghe@inflpr.ro